

The Dynamics of Irreversible Evaporation of a Water–Protein Droplet and the Problem of Structural and Dynamic Experiments with Single Molecules

K. V. Shaitan, G. A. Armeev, and A. K. Shaytan

Moscow State University, Moscow, 119991 Russia

e-mail: shaitan49@yandex.ru

Received December 3, 2015

Abstract—The effect of isothermal and adiabatic evaporation on the state of a water–protein droplet is discussed. The considered problem relates to the design of various approaches for structural and dynamic experiments with single molecules involving X-ray lasers. The delivery of the sample into the X-ray beam is performed by a microdroplet injector in these experiments; and the approach time is in the microsecond range. A version of molecular-dynamics simulation for all-atom modeling of an irreversible isothermal evaporation process is developed. The parameters of the isothermal evaporation of a water–protein droplet that contains sodium and chloride ions at concentrations of approximately 0.3 M have been determined in computational experiments for different temperatures. The *in silico* experiments showed that the energy of irreversible evaporation at the initial stages of the process was virtually the same as the specific heat of evaporation for water. An exact analytical solution of the problem for the kinetics of irreversible adiabatic evaporation has been obtained in the limit of the high heat conductivity of the droplet (or a droplet size not exceeding ~ 100 Å). This solution contains parameters that were derived from simulation of the isothermal evaporation of the droplets. The kinetics of the evaporation and adiabatic cooling of the droplet were shown to be scalable according to the size of the droplet. Estimation of the rate of freezing of the water–protein droplet upon adiabatic evaporation in a vacuum chamber revealed the necessity of using additional procedures for stabilizing the temperature in the droplet nucleus that contains the protein molecule. Isothermal or quasi-isothermal conditions are more favorable for the investigation of macro-molecular structural rearrangements that are related to the functioning of the object. However, the effects of dehydration and a sharp increase in the ionic strength of the aqueous microenvironment of the protein must be taken into account in this case.

Keywords: molecular dynamics, droplet evaporation, water–protein systems, experiments with single molecules, X-ray free electron lasers (XFEL)

DOI: 10.1134/S0006350916020172

Novel methods for the investigation of the structures of biological objects with X-ray free electron lasers are being rapidly developed [1–4]. The prospects of this approach are widely discussed with regard to the fundamental possibility of performing structural experiments with single objects of a protein nature. Importantly, crystallization is not required for such experiments and the temporal resolution can amount to 10 fs. However, sample preparation, the experiment itself, and the interpretation of the X-ray scattering pattern in order to obtain structural information are very complex [5–7]. The following discussion considers the features of the delivery of a macromolecular object to the X-ray beam only, that is, the possible effects of evaporation of water from the water–protein microdroplets which are transported to the measuring chamber from a special injector nozzle [3, 5]. The speed of a sample microdroplet that is released from the injector is in the range of 5–50 m/s; this yields a

flight time of approximately 3 to 30 ms for an approximately 150-mm distance between the nozzle and the beam area. The flight time is long enough for dynamic changes of the protein in the microdroplet to occur, especially in case of single-molecule experiments that require the use of considerably smaller microdroplets than experiments with nanocrystals. Calculations and modeling of the possible changes of the state of the microdroplet at different injection conditions are presented below and the possible effects that can modify the experimental design are discussed.

The problem of droplet evaporation has been discussed for more than a century, since it has multiple thermodynamic, kinetic, hydrodynamic, and other aspects [8–12]. The kinetics of water evaporation (as well as that of the evaporation of other associated liquids) has a some specific features that remain an issue of active discussion [11, 12]. For example the specific evaporation rate may vary in the range of three orders

of magnitude depending on the rather fine details of the setup of an experiment for water evaporation [12]. The protocol of the all-atom molecular simulations for the estimation of kinetic parameters of direct irreversible isothermal evaporation of water from water–protein droplet that is injected into a measuring chamber that does not contain water vapors is developed in the present work. A special design of a computational experiment that includes a spherical trap around the evaporating water molecules is constructed for this purpose. Importantly, direct application of the molecular-dynamics approach to the conditions of adiabatic evaporation requires considerable modification of algorithms that are routinely used for microcanonical NVE- or NPE-ensembles. This is a specific and not simple problem. Here a different approach is developed for the case of adiabatic evaporation. Equations that describe the kinetics of irreversible adiabatic evaporation of the droplet in case of fast equilibration of the temperature (gradient elimination) in the droplet are formulated in the present paper and an exact solution is presented. Estimates that are based on the equation of heat conduction showed that the latter assumption was true for water droplets that are smaller than 100 Å. The exact solution of the equation for adiabatic evaporation contains parameters that can be derived from calculations that characterize the dynamics of isothermal evaporation at different temperatures. These parameters are defined in numerical experiments on the isothermal evaporation of water–protein droplets with a mean initial radius of approximately 35 Å. The solution that is obtained allows scaling of the parameters of the evaporation kinetics for different droplet sizes. The estimation of the parameters' values which was performed using proposed models showed that the delivery of single protein molecules, biopolymers, complexes, or other objects by injection of an aqueous solution into an X-ray beam for structural and dynamic experiments using XFEL requires the calculation of temperature, hydration, and salt concentration effects during the evaporation of water from the microdroplet for selection of an appropriate experimental setup in every individual case. This is especially important for study of conformational dynamics, which is very sensitive to these parameters [13].

Let us consider a simple model of a water–protein droplet that consists of a protein core of radius r_p and an external water layer of radius R . The nature of the protein core is not very important for further analysis if the water layer remains thick enough, as in the computational experiments described below. The equation for irreversible water evaporation from the surface of the droplet in the environment with zero vapor pressure can obviously be formulated as follows:

$$\frac{dN}{dt} = -k(T, N)S(N), \quad (1)$$

where N is the number of water molecules in the droplet, S is the surface area of the droplet at a given number of water molecules, and $k(T, N)$ is the rate of evaporation from unit surface that depends on the temperature T as specified by the Arrhenius law:

$$k(T, N) = k_0 \exp[-h_w(N, T)/k_B T]. \quad (2)$$

The h_w value is usually identical to the value of the enthalpy of vaporization, which depends on the radius of the droplet. This value coincides with the value of the heat of evaporation if the radius is large and decreases due to the excess of surface energy as the droplet size decreases. The decrease is described by the Thomson (Kelvin) formula [14]:

$$\delta h_w \sim \frac{2\sigma v}{R}, \quad (3)$$

where σ is the surface tension (~ 75 dyne/cm for water [14]) or the surface energy in case of small droplets [15], and v is the molecular volume (~ 30 Å³ for water). The δh_w in accordance with (3) and these parameters is approximately $6.5/R$ kcal/mol for R expressed in angstroms. The decrease in activation energy is approximately 0.2 kcal/mol for a droplet radius of approximately 30 Å. The formal assessment for the minimal possible radius of a water cluster, which is of the same order of magnitude as the diameter of the water molecule, gives a value of approximately 2 kcal/mol as a lower estimate of the decrease of the evaporation energy, but application of the formula (3) in this case is hardly justifiable and give the lowest estimate of the effect only. In this limit the value of the heat of evaporation must be of the same order of magnitude as the value for hydrogen bond energy in water (~ 5 kcal/mol if the concept of hydrogen bond can be applied for the water cluster of such small size). The changes in evaporation energy during the variation of the droplet size in the range of several layers of water molecules, as well as the dependence of the heat of evaporation on the number of water molecules in the droplet, will be neglected below and we will consider constant value $h_w = 10.8$ kcal/mol [14]. This is consistent with the results of the molecular simulations that are presented below. The heat of evaporation is weakly dependent on the temperature [14] if the conditions are not close to the critical point. The sublimation energy of water molecules increases approximately by the amount of the specific heat of fusion for ice (~ 1.4 kcal/mol) and gives the value of approximately 12.15 kcal/mol for the transition from the ice to the gas phase. These effects will also be neglected during the analytical assessment and the heat of evaporation h_w in formula (2) will be fixed at the value of ~ 10.8 kcal/mol in all cases.

The preexponential factor in formula (2) shows a weak temperature dependence. The theory of the acti-

vated complex [16] allows for the following representation of this factor:

$$k_0 \sim \frac{k_B T}{h s_w} e^{\delta S/k_B} \sim 0.065 \cdot 10^{13} e^{\delta S/k_B} \text{ s}^{-1} \text{ \AA}^{-2}, \quad (4)$$

where δS is the activation entropy for the transition state of water molecules which are ready to evaporate. Estimates show that this value is approximately three to four times lower than the total entropy of transition of a water molecule from liquid to vapor at normal temperature. The numerical value in the equation (4) corresponds to $T = 310$ K and the surface area per water molecule $s_w \sim 10 \text{ \AA}^2$. Formulas (3) and (4) are of little relevance for further discussion; however, they are useful for the understanding of the general physical nature of the phenomenon (see Fig. 2 below).

The model of concentric spheres gives the following expression (where v is the volume corresponding to a single water molecule):

$$N = \frac{4\pi}{3v} (R^3 - r_p^3); \quad S = 4\pi R^2. \quad (5)$$

Therefore, the decrease of the drop radius during evaporation is characterized by the equation

$$\frac{dR}{dt} = -k(T)v. \quad (6)$$

Let us first consider the isothermal evaporation that occurs after the injection of a water droplet into the dry gas phase at a predetermined temperature and a pressure that is sufficient for efficient energy exchange between gas phase and the droplet. As discussed previously, the evaporation rate constant k is virtually independent of the droplet radius at a constant temperature and a droplet radius that is much higher than the diameter of a water molecule; therefore the solution can be formulated in the following simple way:

$$R = R_0 - kvt, \quad (7)$$

where R_0 is the initial radius. This solution for isothermal evaporation can be easily converted into the number of molecules by using the equation (5). The rate of decrease of the droplet radius at $T = 310$ K and the heat of vaporization at 10.8 kcal/mol is

$$kv \sim 5.3 \cdot 10^5 e^{\delta S/k_B} \text{ \AA/s}. \quad (8)$$

The activation entropy for vaporization can be determined by comparing expression (8) and the evaporation rate determined in a computational experiment.

The molecular dynamics of the process of evaporation of a water–protein droplet was simulated in order to increase the accuracy of the model. A water droplet that included 6259 water molecules and a nucleus that consisted of a lysozyme molecule (length 125 amino-acid residues, PDB code 1JUG, and molecular weight 13.992 kDa) was considered. Thirty sodium ions and 36 chlorine ions were added to the aqueous phase. The

effective concentration of salt in the aqueous phase was 0.29 M. The initial radius of the droplet was approximately 35 Å. Simulations were performed with NAMD 2.9 [17] software package on a Linux cluster containing 64 processor cores. Trajectories analysis was performed with VMD 1.9.2 [18] software package. Data analysis and visualization were performed using in house Python scripts with Scipy and Matplotlib [19] libraries. The system was parameterized in the CHARMM36 force field [20]. Pair non-bonded interactions were treated using the smoothed potential functions with a cutoff radius of 20 Å. Langevin dynamics algorithms (that conserve equilibrium distribution of energy over all degrees of freedom) and the Maxwell distribution of atom velocities at a given temperature were used in the calculation; the step of integration was 1 fs. The length of the trajectories that were obtained at different temperatures amounted to 250 ns and the rate of the recording was 1 frame per 10 ps. A special protocol was designed for the simulation of droplet evaporation dynamics. The C_α atom of leucine 56 was fixed by a soft harmonic potential to prevent the displacement of the entire droplet. The selection of the atom to be fixed did not affect the evaporation process; the considerations that were used for the final selection of the atom included the proximity to the geometric center of the protein and minimal distortion of the nearly spherical droplet mass upon the rotation of the entire water–protein system around the center of mass. Notably, the most commonly used molecular dynamics software does not allow modeling of the movement of molecules over long distances. However, the water molecules that are released upon the evaporation of a water droplet in vacuo are scattered over long distances. The additional limiting potential that trapped the water molecules in a 5 Å-wide spherical zone at a distance of at least 100 Å from the droplet was introduced to enable the modeling of the above-described phenomenon. These limitations prevented the water-molecule coordinates from exceeding the limiting values and did not allow the return of the water molecules to the droplet. The effects of the trapping potential were manifested at distances that exceed the cutoff radius of pairwise interactions; therefore, this potential did not induce changes in the overall behavior of the system.

Water evaporation from the water–protein droplet is illustrated in the graph in Fig. 1. The initial rate of evaporation was 18.7 molecules/ns. The initial effective radius of the droplet fluctuated within the 33–37 Å range. The value of the effective surface area that was determined by rolling a sphere of the radius of 3 Å over the averaged aspherical surface was approximately 24 340 Å². Comparison of these values yields the value of the rate of evaporation:

$$kv \sim 230 \cdot 10^5 \text{ \AA/s}, \quad (9)$$

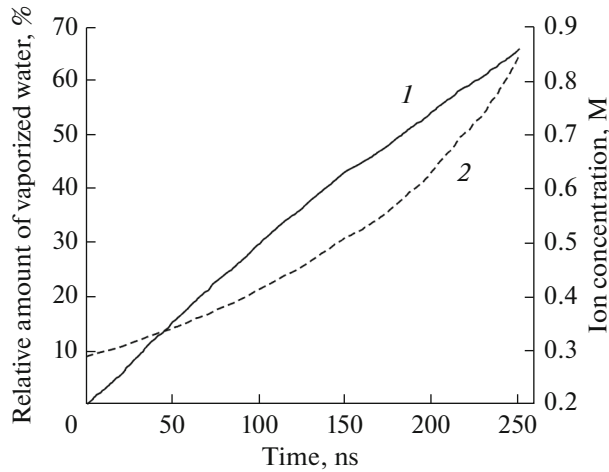


Fig. 1. The time dependence of the relative amount of water molecules that evaporated from water–protein droplets with an average radius of 35 Å (1) and that of the concentration of small ions in such droplets (2) in the case of isothermal evaporation at $T = 310$ K.

which corresponds to the entropy of activation δS of approximately 7.54 cal/(K mol); the total entropy of evaporation for water is approximately 27 cal/(K mol). The result of modeling reveals the existence of a transition zone at the droplet surface. The thickness of this zone was 5 Å or slightly more than the size of a water molecule (Fig. 2) and the density in the zone decreased from the bulk values to zero. This loose surface region apparently makes the contribution to the activation entropy.

Simulation of droplet evaporation at various temperatures (Fig. 3) leads to the value of activation energy for evaporation close to 10.76 kcal/mol; this is very similar to the values for the macrovolume [14] which was discussed above.

The radius of the droplet can theoretically decrease to zero within 1.5 μs if the evaporation rate $k(T)$ remains constant. Near this time the existence of the droplet itself appears problematic. The use of larger droplets may result in increased complexity of interpretation of the scattering pattern of individual protein molecules due to the increase of the scattering centers number. On the other hand, complete evaporation of a droplet with a radius of 70 nm takes approximately 30 μs under these conditions. There is another problem that is worth mentioning. The increase of the salt concentration in the aqueous phase surrounding the protein molecule is illustrated in Fig. 1. Molecular dynamics simulations reveal the absence of ion capture by water molecules upon evaporation. The increase of the salt concentration to a certain level is expected to increase the heat of evaporation considerably due to fixation of the water molecules in the solvation shells of the ions. Thus, conservation of the water phase in the microdroplets at a specific concen-

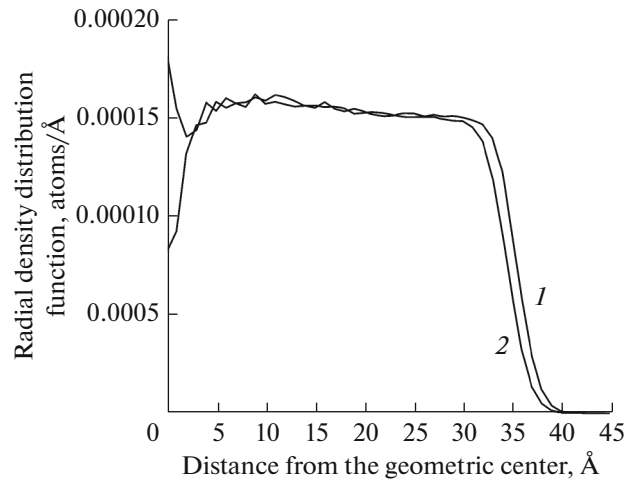


Fig. 2. The radial density distribution function for a water–protein droplet relative to the geometric center of the droplet at 0 ns (1) and 30 ns (2) from the start of evaporation. Density fluctuations in the central part of the droplet are due to movements (rotation) of the entire droplet and the contribution of the lysozyme molecule to the density.

tration of salt in the solution is theoretically possible. The dramatic effects of high ionic strength on protein structure and dynamics are among the disadvantages of this approach. Injection of the droplets into the gas phase with a sufficiently high partial pressure of water vapor may be an alternative, although this approach has some drawbacks as well. The study [21], which addressed the molecular dynamics of the effects of the water and salt environment on lysozyme, is worth mentioning here.

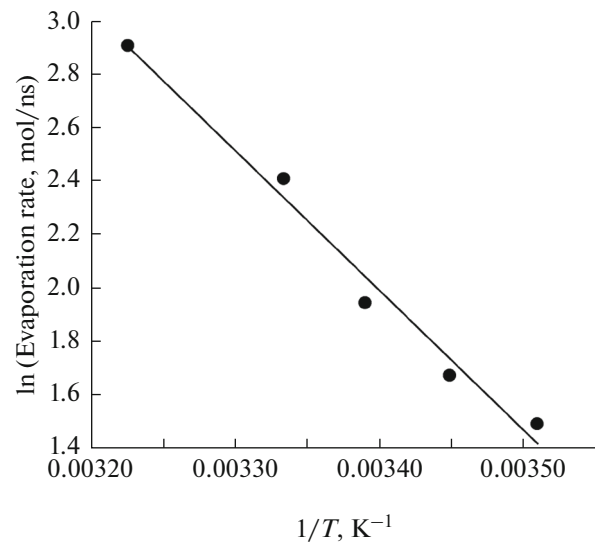


Fig. 3. The temperature dependence of the initial water evaporation rates for water-protein droplet with an average radius of 35 Å. Activation energy (specific heat of vaporization) obtained from linear approximation in the Arrhenius coordinates is 10.76 kcal/mol.

Let us then consider the process of adiabatic evaporation of water from microdroplets injected into a vacuum chamber, since this process is most likely to occur during an experiment. Water evaporation will cause cooling of the microdroplets in this case.

Let us first estimate the possible effects of temperature inhomogeneity in the microdroplet. The thermal conductivity λ of a (water) droplet is approximately $1.5 \cdot 10^{-3}$ cal/(cm s K) [14]. If the linear size L of the droplet is estimated at 70 Å, the assessment of the characteristic time τ of the temperature-gradient equilibration related to a water molecule evaporation from a droplet leads to the value of approximately $0.34 \cdot 10^{-9}$ s. The estimate is based on the equation of heat conductivity:

$$\tau \sim \frac{L^2}{\lambda} \rho C_w, \quad (10)$$

where $\rho \sim 1$ is the density of the droplet and $C_w \sim 1$ cal/(g K) is the specific heat capacity of water [14]. Thus, at the droplet cooling rate dT/dt significantly lower than $\delta T/\tau \sim 10$ K/ns (where δT is the acceptable temperature change of approximately 3 K that does not have a pronounced effect on the structure and dynamics of a droplet) one may assume that the state of the droplet is close to thermal equilibrium and use thermodynamic estimates for the assessment of droplet freezing effects upon adiabatic evaporation of water.

The corresponding equation that connects the cooling rate and the rate of evaporation can be derived from the following considerations. The change of microdroplet enthalpy δH due to the evaporation of δN molecules of water ($\delta N \ll N$) should be almost equal to the decrease in enthalpy due to cooling by δT ($\delta T \ll T$):

$$\delta H(N, T) \approx h_w(N, T) \delta N / N_A = C_p(N, T) \delta T, \quad (11)$$

where $h_w(N, T)$ is the heat of water evaporation (per mole) from a droplet containing N water molecules at the temperature T , and N_A is Avogadro's number. The specific heat of evaporation will be assumed independent of the temperature (far from the critical point) and the number of water molecules (that is, the radius of the droplet). The heat capacity $C_p(N, T)$ of the water–protein droplet is a sum of the heat capacities of the protein molecule and the water shell:

$$C_p(N, T) = \frac{C_{pr}(T) M_{pr}}{N_A} + N \frac{18 C_w(T)}{N_A}, \quad (12)$$

$C_p(N, T) \sim N C_w$ is the heat capacity of the water–protein droplet. The water specific heat capacity C_w decreases by approximately two times upon the transition through the water freezing point and then decreases gradually with decreasing T , so that the value at $T = -100^\circ\text{C}$ is approximately 1.5 times lower than at the freezing point. $C_{pr} \sim 0.3 T / 300$ cal/(g K) is the heat capacity of the protein (at temperatures higher than 50 K) [22], and M_{pr} is the molecular

weight of the protein (approximately 14000 Da for lysozyme). The state of the water–protein droplet changes due to water evaporation and temperature decrease. Further assessments of the kinetics of adiabatic evaporation in a relatively narrow temperature range (from 310 to 200 K) will be performed using a temperature-independent value for the heat capacity of the droplet. The contribution of the protein molecule to the heat capacity of the droplet will be neglected, and the efficient radius of the protein molecule in the expression (5) will be assumed to be much lower than the radius of the droplet.

Transformation of the equation (11) under the conditions described above gives two expressions that are useful for the subsequent analysis

$$\frac{d \ln N}{dT} = \frac{1}{T_w} \quad (13)$$

and

$$\frac{d \ln N}{dt} = \frac{1}{T_w} \frac{dT}{dt}, \quad (14)$$

where

$$T_w = \frac{h_w}{18 C_w} \approx 600 \text{ K} \quad (15)$$

is the ratio of the specific heat of evaporation to the specific heat capacity, which is a parameter with the dimension of temperature that characterizes the composition of the droplet.

Equation (13) leads to the conclusion of fundamental importance concerning the existence of the highest limit of the decrease of the number of water molecules in a drop upon adiabatic evaporation:

$$\frac{N}{N_0} \geq \exp\left(-\frac{T_0}{T_w}\right); \quad \frac{R}{R_0} \geq \exp\left(-\frac{T_0}{3T_w}\right). \quad (16)$$

Note that $N \sim R^3$ and equations (13) and (14) can be easily formulated in terms of the droplet radius. These expressions can be used to show that, for example, the relative number of water molecules that remain in a droplet that is cooled to absolute zero from an initial temperature of 300 K during adiabatic evaporation within an infinite time interval will be $e^{-1/2} \sim 0.6$. The droplet radius will only change by approximately 15% in this case.

Importantly, equation (6) for the kinetics of evaporation is also correct if the droplet temperature is time dependent, although the dependence of T on time should be taken into account in this case and the solution cannot be expressed in the simple form (7). However, a solution for evaporation kinetics can be formulated in quadrature in this case. For this, let us consider the relationship between the droplet radius and the temperature derived from (13)

$$T = T_0 - 3T_w \ln R_0/R \quad (17)$$

or

$$R(t) = R_0 \exp[(T(t) - T_0)/3T_w]. \quad (17a)$$

Substitution of (17) in eq. (6) and separation of the variables yields

$$\int_R^{R_0} \frac{dR}{k[T(R)]v} = t. \quad (18)$$

The weak temperature dependence of the pre-exponential factor in $k(T)$ can be neglected; taking into account (2) we obtain

$$t = \frac{R_0 e^{-a_0}}{b_0 k(T_0)v} \int_0^\lambda \exp\left(-\frac{\lambda}{b_0} + \frac{a_0}{1-\lambda}\right) d\lambda, \quad (19)$$

where are dimensionless parameters

$$\lambda = b_0 \ln R_0/R, \quad a_0 = h_w/k_B T_0, \quad (20)$$

$$b_0 = 3T_w/T_0.$$

The integral (19) gives the precise solution of the problem of adiabatic evaporation of a droplet for the assumptions that are listed above. The value of the droplet temperature at a given time (or radius) is defined by an obvious expression (with (17) taken into account):

$$T = T_0(1 - \lambda). \quad (21)$$

The time dependence of the droplet temperature is described by an equation that is obtained by substituting the upper limit value that was obtained from (21) to the integral (19).

At $T \sim T_0$ ($\lambda \ll 1$) the second term in the exponent (20) can be expanded in a power series of λ . Keeping the linear terms only yields

$$T = T_0 - \frac{3T_w}{a_0 b_0 - 1} \ln[1 + (a_0 b_0 - 1)t/\tau_i]. \quad (22)$$

Comparison with (17) leads to the following expression for the droplet radius:

$$R = R_0[1 + (a_0 b_0 - 1)t/\tau_i]^{-1/(a_0 b_0 - 1)}, \quad (23)$$

where

$$\tau_i = \frac{R_0}{k(T_0)v} \quad (24)$$

is the time of isothermal evaporation of the droplet at the starting temperature derived from (7).

By using the droplet parameter values that were applied in the present study (initial radius 35 Å, initial temperature 310 K) we obtain the following: $a_0 \sim 17.42$ and $b_0 \sim 5.8$. The time of isothermal evaporation (25) is close to 1522 ns and shows a linear dependence on the initial droplet radius, as one can demonstrate using (9).

The kinetics of the temperature change in the droplet that is under consideration is described by the following integral (with t expressed in ns)

$$t = 7 \cdot 10^{-6} \int_0^{1-7/310} \exp\left(-0.172\lambda + \frac{17.42}{1-\lambda}\right) d\lambda. \quad (25)$$

At T values close to the initial temperature, one can use the asymptotic formula (22):

$$T(t) \sim 310 - 17.97 \ln(1 + 0.0657t) \\ \sim 310 - 1.18t, \text{ K.} \quad (26)$$

Let us remember that time is expressed in nanoseconds. The initial cooling rate (at $0.0657t \ll 1$) of a droplet that contains 6249 water molecules is approximately 1.2 K/ns, so that the emergence of a state similar to heat equilibrium can be assumed for such a droplet according to the estimate that was performed above (10). The following expression for R can be formulated using (23):

$$R(t) \sim 35(1 + 0.0657t)^{-0.01} \\ \sim 35(1 - 0.657 \cdot 10^{-3}t), \text{ \AA.} \quad (27)$$

The formulas also show that the cooling rate of a droplet that is undergoing adiabatic evaporation is halved after 15 ns, reduced threefold at 30 ns, and so on. Notably, these approximations cannot be used for long time intervals due to the constraints (16) and $T > 0$.

Graphs that illustrate the solutions of the temperature, radius, and approximations (26) and (27) are shown in Fig. 4.

The t values for the transition region that are most relevant for X-ray laser experiments range from 10^3 to 10^4 ns; the estimated temperature of the droplet ranges from 250 to 230 K. The relative decrease of droplet radius is only $\sim 5\%$ under these conditions. (Notably, expression (25) yields a time of approximately 30 billion years, or longer than the lifetime of the universe, for cooling to 100 K, whereas the decrease of the drop size will be close to the extreme value that is derived from formula (16), or approximately 15%, in this case. Quantum corrections must be taken into account when time intervals of the aforementioned duration are considered).

Equation (23) demonstrates the existence of two stages of cooling during the adiabatic evaporation of droplets. The rate of droplet cooling at the initial stage that lasts for several tens of ns is almost equal to the initial rate of approximately 1.2 K/ns (see above for the expressions that were used to determine this value). The evaporation rate, as well as the rate of droplet cooling, starts decreasing in the temperature range of 300–280 K (10–100 ns) and the cooling kinetics assumes a logarithmic character. The difference between the exact formula (25) and the asymptotic expression exceeds 5 K at times that exceed 1000 ns (Fig. 4).

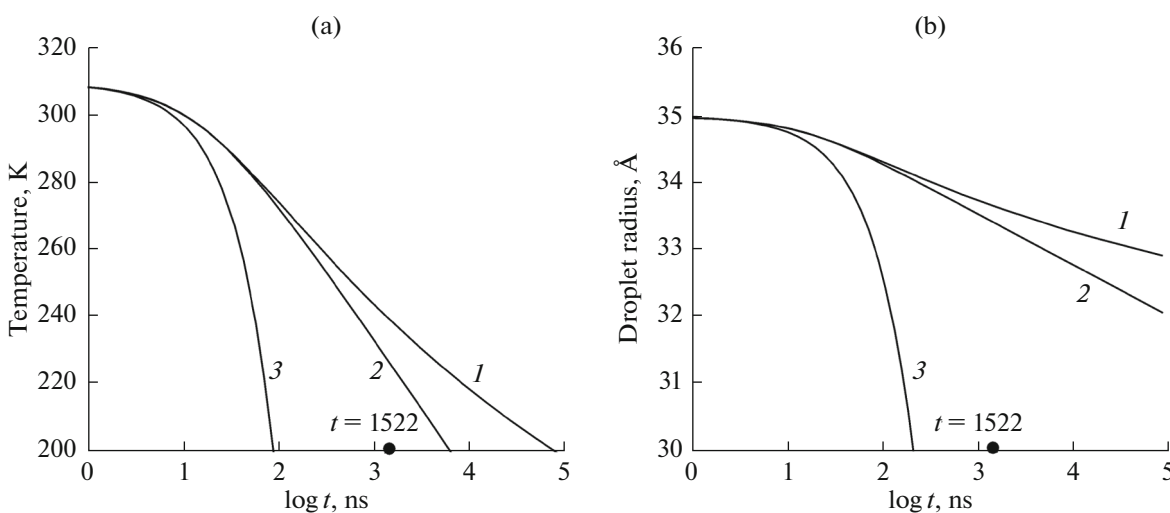


Fig. 4. The time dependences of the temperature (a) and the radius (b) of a droplet under investigation during adiabatic evaporation: 1—the exact solution (25), 2—an asymptotic curves (26) and (27), 3—a linear approximation of the asymptotic curves. Dependence 3 for $R(t)$ corresponds to a linear change in the droplet radius upon isothermal evaporation as well. The 1522 ns point on the time axis corresponds to the time of the complete evaporation of the droplet in an absolutely dry environment under isothermal conditions.

The time of isothermal evaporation (24) is the only parameter that depends on the initial droplet size in the formula (22). This fact is especially worth mentioning. Thus, a tenfold increase of droplet size will lead to a tenfold increase of the duration of the cooling process. A similar dependence will be observed in the case of the relative change in the droplet radius according to formula (23); however, the characteristic time of thermal equilibration (10) will increase by a hundred times. Therefore, one can expect that the evaporation (cooling) kinetics of large droplets with a radius that exceeds 10 nm will be more complex due to rapid freezing of the surface layers. Equations that describe evaporation and heat conductivity must be conjugated to find a solution of this problem. A qualitative manifestation of this effect will consist in a smoother character of the dependence of the time parameter (24) on droplet size in the case of droplets with larger radii. The hypothetical case of a sharp increase of the thickness of the hydration shell (by approximately 1000 times) can also be considered with regard to stabilization of the temperature of the protein core of the droplet. The penetration depth of temperature changes that are related to heat conduction will be close to 2 μm at the flight time of 30 μs , as can be shown using expression (10). Preparation of micrometer-size droplets that contain a single protein molecule per droplet is obviously a complex task.

Thus, cooling of the droplets is the major effect that is expected to occur upon the injection of microdroplets that form at room temperature into a vacuum-measuring chamber. The decrease of droplet temperature during a time interval with a duration of the order of 10 μs (the time of the transition from the

injector to the measurement zone) is expected to range from 50 to 100 K and the relative loss of water by evaporation is expected to be close to 5%. The ionic strength of the solution that surrounds the protein is also expected to increase to the same degree. Temperature effects may alter the conformational dynamics parameters of the protein to a considerable extent and possibly induce changes in the structure of macromolecular complexes. The effects that are considered in the present study must be taken into account during the planning of experiments that employ X-ray free electron lasers in order to characterize the structure and dynamics of single molecular objects. It is important to perform detailed calculations of the changes of the thermodynamic characteristics of the droplets that occur during the experiment. The development of dedicated tools and techniques may be necessary to stabilize these characteristics. The use of isothermal conditions makes the situation more predictable, while the requirement for maintaining efficient heat transfer, as well as the sharp increase in the ionic strength of the medium upon rapid evaporation of the droplets, increases the complexity of the experimental setup in this case. A chamber filled with water vapor at a saturating pressure can be considered as an alternative in this case. The results of the calculation of temperature effects are easily predictable if nanodroplets smaller than 10 nm are used. Adiabatic evaporation of water from droplets of micrometer and submicrometer sizes apparently results in the formation of a non-stationary temperature gradient field around the macromolecule; this may lead to poorly characterized structural and dynamic effects.

ACKNOWLEDGMENTS

This work was supported by the Ministry of Education and Science of the Russian Federation (molecular modeling, contract no. 14.616.21.0003) and the Russian Foundation for Basic Research (analytical solutions, grant no. 15-29-04856).

REFERENCES

1. M. M. Waldrop, *Nature* **505**, 605 (2014).
2. J. Hajdu, *Curr. Opin. Struct. Biol.* **10**, 569 (2000).
3. H. N. Chapman, P. Fromme, A. Barty, et al., *Nature* **470**, 73 (2011).
4. K. V. Shaitan, M. P. Kirpichnikov, V. S. Lamzin, et al., *Vestn. RFFI No. 4* (80), 38 (2013).
5. U. Weierstall, J. C. H. Spence, and R. B. Doak, *Rev. Sci. Instr.* **83**, 035108 (2012).
6. R. Fung, V. Shneerson, D. K. Saldin, et al., *Nat. Phys.* **5**, 64 (2009).
7. A. Barty, J. Kopper, and H. N. Chapman, *Ann. Rev. Phys. Chem.* **64**, 415 (2013).
8. O. Knacke and I. N. Stranskii, *Usp. Fiz. Nauk* **68** (2), 261 (1959).
9. A. V. Kozyrev and A. G. Sitnikov, *Usp. Fiz. Nauk* **171** (7), 765 (2001).
10. N. A. Fuchs, *Evaporation and Droplet Growth in Gaseous Media* (USSR Acad. Sci., Moscow, 1958; Pergamon, London, 1959).
11. I. W. Eames, N. J. Marr, and H. Sabir, *Int. J. Heat Mass Transfer* **40**, 2963 (1997).
12. R. Marek and J. Straub, *Int. J. Heat Mass Transfer* **44**, 39 (2001).
13. A. B. Rubin, *Biophysics*, Vol. 1: *Theoretical Biophysics* (Inst. Comput. Res., Moscow, 2013) [in Russian].
14. N. B. Vargaftik, *Handbook of Physical Properties of Liquids and Gases* (Nauka, Moscow, 1972; Springer, Berlin, 1975).
15. J. Frenkel, *Kintic Theory of Liquids* (USSR Acad. Sci., Moscow, 1945; Clarendon, Oxford, 1946).
16. S. Glasstone, K. J. Laidler, and H. Eyring, *The Theory of Rate Processes* (McGraw-Hill, New York, 1941; Gos. Izd. Inostrannoi Literatury, Moscow, 1948).
17. J. C. Phillips, G. Zheng, S. Kumar, and L. V. Kale, in *ACM/IEEE 2002 Conference* (2002) p. 36.
18. W. Humphrey, A. Dalke, and K. Schulten, *J. Mol. Graph.* **14**, 33 (1996).
19. J. D. Hunter, *Comput. Sci. Eng.* **9**, 90 (2007).
20. J. Huang and A. D. MacKerell, Jr., *J. Comp. Chem.* **34**, 2135 (2013).
21. I. L. Kanev, N. K. Balabaev, A. V. Glyakina, et al., *J. Phys. Chem. B.* **116**, 5872 (2012).
22. G. M. Mrelvlishvili, *Usp. Fiz. Nauk* **128** (2), 273 (1979).

Translated by S. Semenova